Supporting information

Surface-Induced Conformational Changes in Doped Bovine Serum Albumin Self-Assembled Monolayers

Edith Beilis[1,2], Bogdan Belgorodsky[2], Ludmila Fadeev[2] , Hagai Cohen[4], Shachar Richter*[1, 3]

[1] University Center for Nanoscience and Nanotechnology, [2] School of Chemistry, Raymond and Beverly Sackler Faculty of Exact Sciences, [3] Department of Materials science and engineering ,Tel Aviv University, Tel-Aviv, Israel [4] Department of Chemical Research Support, Weitzman Institute of Science, Rehovot, Israel.

1. Experimental and Materials

1.1 Materials

Purified Bovine serum albumin (BSA, fraction V, lyophilized powder) was purchased from Sigma Aldrich and used as received. Sodium Phosphate Buffer was prepared using sodium salts: sodium phosphate monobasic and sodium phosphate dibasic to give pH 7.2 (200mM) at room temperature. The buffer stock solution was diluted prior to use with deionized water (resistivity 18.2 Ωcm). Stock protein solution in buffer were prepared immediately before use. 5,10,15,20-Tetraphenyl-21H,23H-porphine copper(II) (TPP-Cu), 5,10,15,20-Tetraphenyl-21H,23H-porphine iron(III) chloride (TPP- FeCl), and 5,10,15,20-Tetraphenyl-21H,23H-porphine (TPP), purchased from Sigma Aldrich were used as received. Stock solutions of the three compounds dissolved in Dimethyl Sulfoxide (DMSO) were prepared immediately before use. TPPFeCl solubility in DMSO/Buffer mixture was the best resulting in a homogenous solution. On the other hand, TPP and TPPCu formed semi-homogunous suspensions with some aggregation observed. To improve the homogeneity, all the solutions were sonicated prior to incubation with BSA

1.2 Preparation of doped BSA (solution)

The doped BSA complexes were prepared by adding TPP derivatives (stock solutions in Dimethyl Sulfoxide, DMSO) to BSA (stock solution in aqueous phosphate buffer, pH 7.2 10mM), at a fixed molar ratio 5:1, respectively. Following incubation (over night - 24 hours at room tempreture) the doped BSA solutions were separated and purified using a Sephadex G-25 gel permeation column (Pharmacia Biotech) with phosphate buffer (10mM, pH 7.2). The size exclusion chromatography step was used to remove TPP derivatives aggrgates from doped BSA buffered solution.

1.3 Preparation of Gold-coated surfaces

N-type silicon <100> wafers, with 100nm thermally grown silicon oxide, resistivity (0.019-0.022Ωcm) were used as substrates. Gold films were prepared by e-beam evaporation using a VST-TFDS-680 thin film deposition system: titanium (Ti) was used as adhesion layer, thickness 15nm (rate: 0.7A/sec) followed by evaportion of Gold (Au) layer, thickness 150nm (rate: 1A/sec). During Evaporation the sample is kept at room temperature.The samples were then annealed at 345° in a vaccum oven for 3-6 hours.

1.4 Preparation of self-assembled monolayers (SAMs)

Monolayers of un-doped-BSA and the three differently doped BSA complexes were prepared on annealed hydrophilic gold. Clean hydrophilic gold samples were prepared by ultrasonication in acetone followed by isopropanol and rinsing with DI water. The samples were then dried with nitrogen flow and placed in a UV-Ozon cleaner for 15 min. The clean gold surfaces were hydrophilic as expected. Subsequently, the gold samples were immediately immersed in BSA or the differently doped-BSA complexes buffered solutions for 20h. After which the samples were removed from solution rinsed with DI water and dried with nitrogen flow. The procedure used for monolayer preparation was based on procedures previously employed for prepartion of un-doped BSA monolayers directly on gold.

2. UV-Vis absorption measurements

The UV-visible spectra were perfomed on a Cary 5000 (Varian) at 200-800nm (1.0nm steps), using a 10mmx4mm qurtz cuvette. Baseline was corrected with respect to the phospahte buffer solution pH 7.2, 10mM .

3. Steady state fluorescence measurements

Fluorescence spectra were measured on a Flurolog-322 spectrometer (John Yvon). The fluorescence of BSA was measured by excitation at λ=280 nm (corresponding to the maximal absorbance measured by UV-Vis). Emission of BSA was recorded at 290-500 nm spectral range (1nm steps), using a 10mmx4mm qurtz cuvette.

4. Docking simulations

Docking models were obtained using the patchdock algorithm [1]. In our simulation, the initial coordinates of the X-ray structure of the BSA dimer were obtained from the Protein Data Bank (PDB ID: 3V03) from which crystallographic water molecules were removed. The coordinates of the TPP ligand were obtained by geometry optimization and DFT energy minimization calculations (Gaussian 03® software). The final structure of the complex was estimated by application of the patchdock algorithm which included the BSA and the relaxed TPP.

4.1 Representative images of patchdock simulations of TPP doped BSA

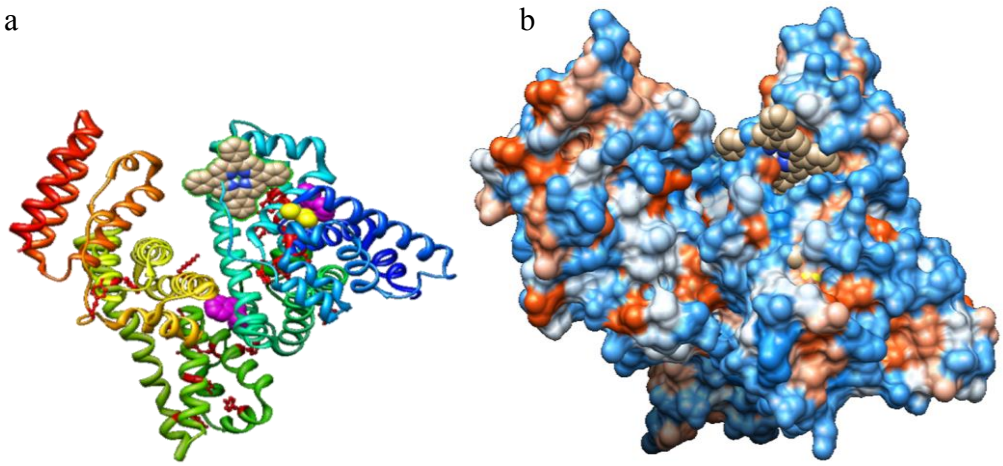

Figure S1: patchdock simulation of TPP doped BSA shows the protein's sub-domains; a) shows the TPP molecule located in sub-domain IB in close proximity to Trp 135 (highlighted in pink) and the Cys34 residue (highlighted in yellow), tyrosine residues (highlighted in red). b) Shows the protein's hydrophobic surface and the TPP molecule in a hydrophobic slot in sub-domain IB.

5. AFM imaging

AFM measurements were performed using both (i) Agilent pico-plus AFM and (ii) JPK NW III AFM.

(i) Agilent pico-plus AFM: The images were taken using tapping mode with a NSC18 / Al BS (Umasch) tip force constant (2.8 N/m) with typical resonance frequency of 75kHz (ii) JPK NW III AFM: TPP doped BSA self-assembled on gold was scanned with a higher constant force tip (40 N/m), typical resonance frequency 325kHz (NSC15 / Al BS umasch). Image analysis was done WSxM® software[2]. Image processing was done by using the flatting (default: offset) and equalize (default) functions of the WSxM® software.

5.1 SAMs surface morphology analysis

Analysis of the AFM images revealed that the surface RMS and average roughness decreased as the BSA molecules adsorbed to the annealed gold surface (Figure S2, Table S1). Protein molecules are substantially softer than the gold grains, therefore the decrease was attributed to the formation of BSA SAMs. The differences in RMS roughness between un-doped BSA and TPP doped BSA are attributed to surface coverage differences between the SAMs. The doped BSA SAMs form a loosely packed monolayer with exposed gold grains between the protein molecules (as will be shown by XPS as well), resulting in an increase in the RMS roughness compared to un-doped BSA. To observe BSA molecules directly, an atomically flat surface is required, however the use of annealed gold as a substrate facilitated distinguishing between the gold grains (lateral size ~200 nm) and the proteins molecules and aggregates (max ~35 nm, due to tip-sample convulotion).

Table S1: Summary of AFM images analysis using WSxM® software[2]

Measurement Sample	Gold after Evaporation	Annealed gold	BSA	TPP doped BSA
RMS roughness	1.86	1.17	0.95	1.03
Peak to peak height	7.56	4.99	3.96	4.23
Roughness average	1.51	0.90	0.77	0.84
Average height	3.78	2.48	1.99	2.11

5.2 Protein orientation (based on simple adsorption model)[3]

To asses the BSA orientation towards the surface a simple adsorption model[3] is suggestedd based on the AFM measurements: Assuming un-doped BSA molecules distort upon adsorption (creating a close packed monolayer) from their compact pH depended conformation in solution to a prolate ellipsoid, (r_2=14nm , r_1=r_3=4nm), the average height of the protein SAM, h, can be estimated. h is defined as the ratio between the volume (V= (4/3) π $r_1^2 r_2$) and footprint area (A= π $r_1 r_2$) of the adsorbed BSA molecule. The volume (V) of the BSA molecules is constant and equals 117 nm^3 . However the "footprint" (A) is depended on the molecules orientation towrads the surface. For "side on" adsorption of BSA, A_{sideon} equals 44nm^2 , therefore, h is approximated as 2.7nm. For "end on" adsorption of BSA, A_{endon} equals 13nm^2, therefore, h is approximated as 9nm. The measured average height obtained from our experimental results suggested that BSA produces a "side-on" monolayer on gold surface.

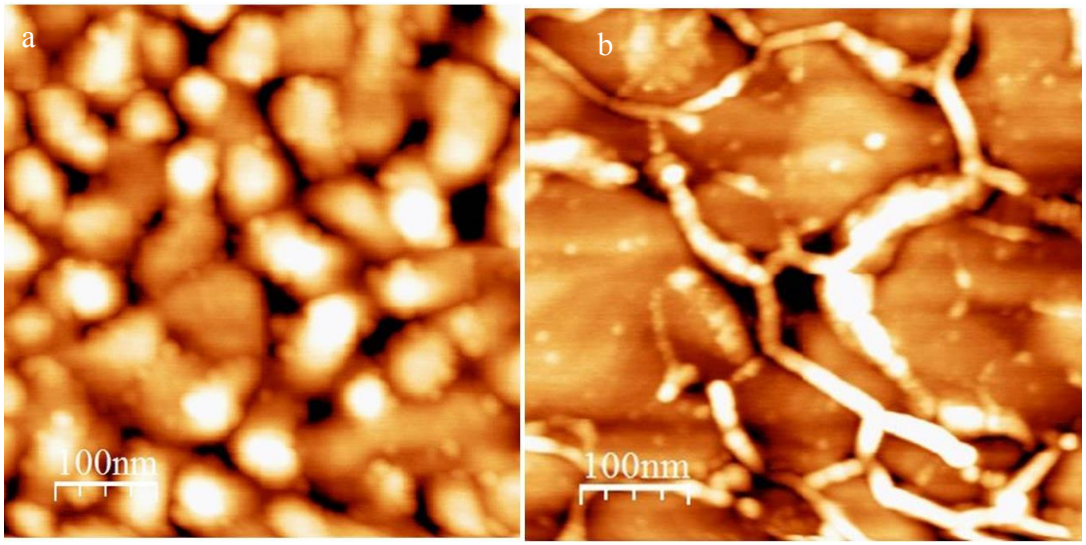

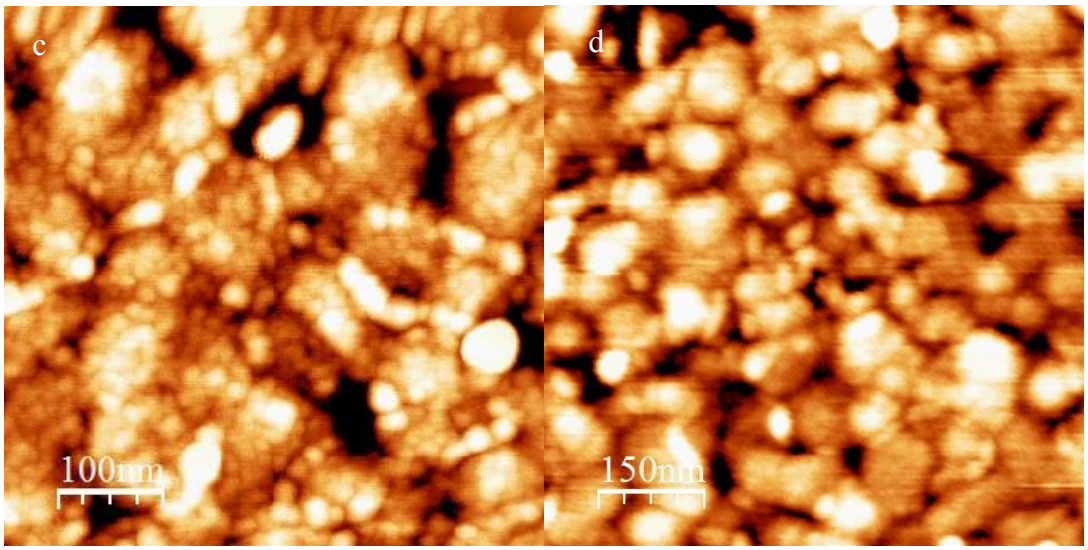

Figure S2: (a) As deposited gold z= 7.56nm (b) annealed gold z=4.99 nm (c) Un-doped BSA 1mg/ml SAM z=3.96 nm (d) TPP doped BSA SAM z=4.23nm

6. XPS measurements

The XPS measurements were performed using both Kratos AXIS-HS and Kratos Ultra-DLD spectrometers with monochromatic Al Kα source (1486.6eV) at low power, 75 W, and base pressure $<10^{-9}$ torr.

6.1 SAMs average thickness estimation:

Organic overlayer thickness estimation is based on the attenuation of photoelectrons across an ideal uniform overlayer. Relying on previous experience at the Weizmann surface laboratory, an average attenuation parameter (λ) of 33A is used here for the photoelectrons traversing the organic layer[4,5].

Table S2: Estimated layer thicknesses (in Å) and the corresponding gold atomic concentrations (%), as derived from the XPS data of self-assembled un-doped and doped BSA SAMs. Data is complementary to Table 1 in the manuscript. The experimental relative error here is < 15% .

	Au 4f (%)	d (Å)
Un-doped BSA	23.4	48
TPPFeCl doped BSA	27.4	43
TPPCu doped BSA	31.2	39

6.2 Angle resolved XPS of the Sulfur (S 2p) line

Fig. S3**Error! Reference source not found.** shows representative angle resolved spectra of the sulfur (S 2p) line, taken for undoped BSA SAMs on gold. Several S components are resolved (binding-energy values are given for the $2p_{3/2}$ peak):

1. unbound BSA components (~163.5eV)
2. S-metal (161.2 &162.1 eV), originated from the cysteine –Au bond and, possibly, other moieties directly bound to the substrate. The angle dependence of this component proves its relatively deep location (see Fig. S3,a).
3. Oxidized S (168.5 eV) – In doped BSA this component may possibly arise from the solvent DMSO residual molecules; however, it is stressed that the related DMSO amount (<1% of the total oxygen content) is far from accounting for all the extra oxygen (~30% of the total O content).

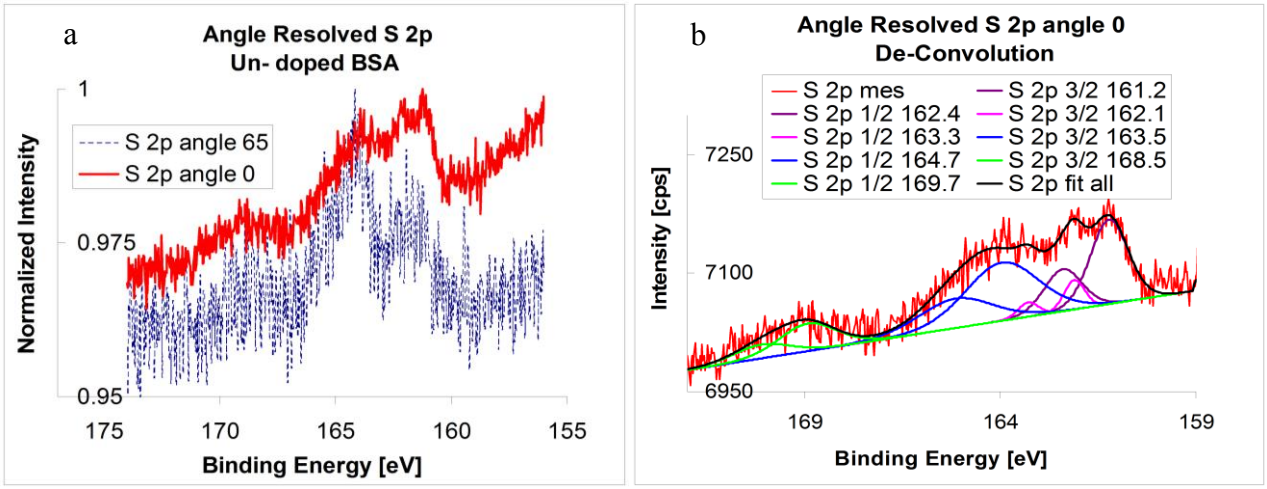

Figure S3: High resolution S 2p spectra of un-doped BSA SAM on Gold: a) at two representative take-off angles with respect to the surface normal (0-red and 65-light bule); b) an example of the components obtained by the curve fitting procedure. Note the suppression at high take-off angles (panel a) of the S-Au components (around 162 eV).

Table S3: The extracted S(2p) components: binding energies (in eV) and relative intensities (in atomic %), attributed to: sulfur bound to gold, BSA S-S and S-C bonds, and oxidized sulfur, as derived at normal take-off angle. The relative error here is ≤ 20% .

Sample / Signal	Bound 161.2 [eV] 162.1 [eV]	Un bound 163.5 [eV]	Oxidized 168.5 [eV]
Un-doped BSA	39.30%	44.43%	16.28%
TPPCu doped BSA	41.24%	39.63%	19.11%
TPPFeCl doped BSA	47.91%	34.94%	17.16%

6.2 Angular dependence of the O (1s) XPS line

Error! Not a valid bookmark self-reference. shows the Oxygen (O 1s) line at representative take-off angles , taken for undoped and doped BSA SAMs on gold. One observes a significant change in relative intensities of the dominant components in this line, as a function of take-off angle. Supported by the full quantitative analysis, see Tables 1 and S4, we propose the following assignment :

1. The low-energy component (~530 eV) for which the intensity decreases at grazing angles, is associated with signals of species located near the inner interface. This O-component varies quite much from sample to sample and is attributed mainly to oxidation at the gold surface due to the cleaning treatment by UV irradiation and Ozone prior to adsorption. Partially, it may also arise from minor Ti-diffusion to the top surface, found to take place occasionally during the annealing process, before protein assembly. Importantly, this diffusion was found to have no significant effect on the BSA or doped BSA coverage. Moreover, our conclusions on excess oxygen and dehydration of un-doped BSA remain similarly valid after subtraction of the interface oxygen component.

2. Two higher-energy Oxygen components constitute the main peak around 532 eV, both associated with molecular layer species: (1) O within the protein (at ~531.9 eV) and (2) bound water (at ~533 eV).

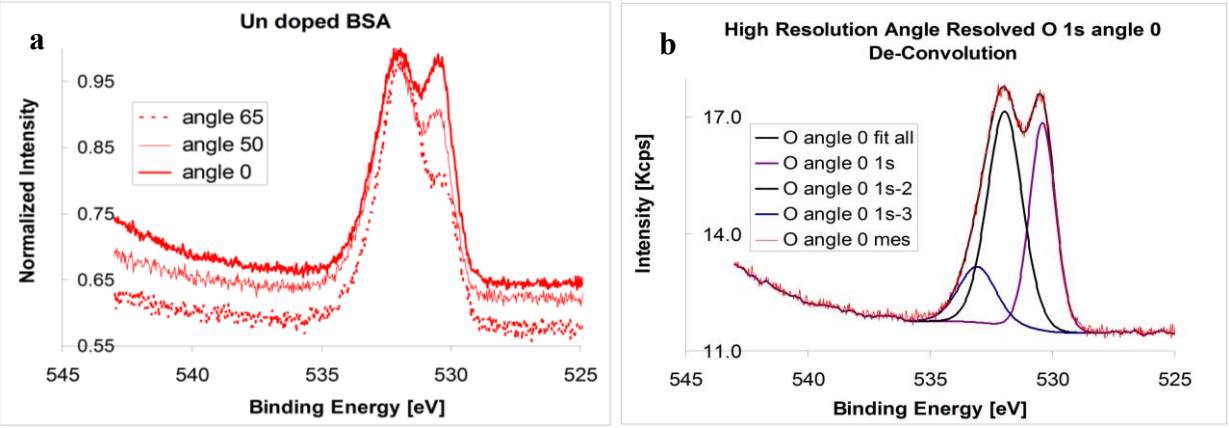

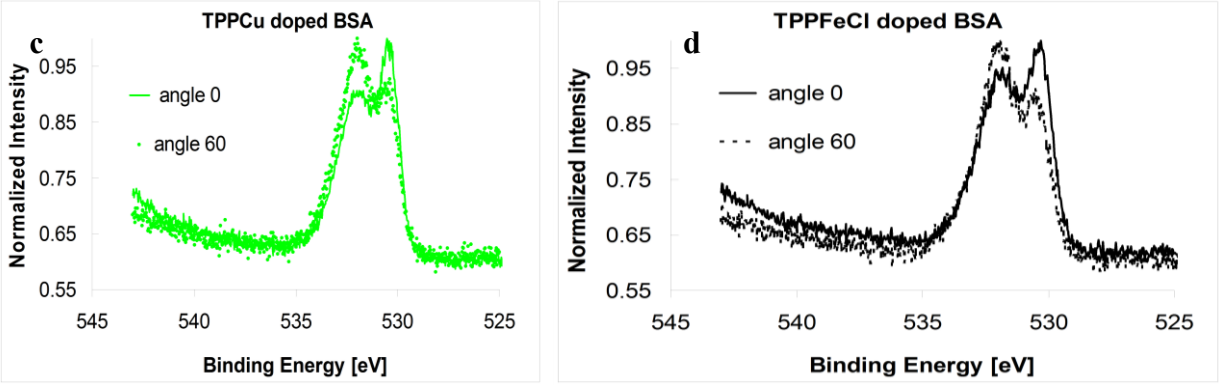

Figure S4 High resolution angle resolved spectra of Oxygen (O 1s) a) un-doped BSA (red) b) an example of the components obtained by the curve fitting procedure c) TPPCu doped BSA (green) d) TPPFeCl doped BSA SAMs on gold (black)

Table S4: The relative intensities of O (1s) components in doped BSA SAMs, as derived from the angle-dependent XPS: O_1 (at 530.3 eV) is the component originating from species at the interface with the gold substrate; O_2 (around 532 eV) sums over various monolayer-related species, including the BSA oxygen and the bound water. The relative error here is ≤ 15% .

sample		TPPCu doped BSA	TPPFeCl doped BSA
Take off angle	Signal	Concentration [%]	Concentration [%]
60°	O_1	30.79%	33.28%
	O_2	69.22%	66.72%
0°	O_1	38.48%	40.03%
	O_2	61.52%	59.98%

6.4 A note on Porphyrin aggregation in buffer solution

Further analysis of the XPS measurements indicated traces of excess metal ions (Cu, Fe) in the different SAMs, as given in Table S5. We cannot exclude the option of having more than one dopant molecule on each BSA molecule. Yet, it is also possible that along the lignad-BSA complexses, TPP-metal aggregates were adsorbed at exposed gold areas between the BSA molecules.

Table S5: Theoretical and XPS-derived atomic concentrations of un-doped and doped BSA SAMs, normalized to the nitrogen content. The theoretical values are obtained for 1 TPP molecule bonded to each BSA molecule.

SAMs		Cu/N	Fe/N
Doped BSA	Theoretical*	0.0013	0.0013
TPPFeCl doped BSA	Measured	0.04	-------
TPPCu doped BSA	Measured	--------	0.009

7. PMIRRAS measurements

PM-IRRAS spectra were recorded using Bruker optics PMA50 external module in conjunction with a Vertex 70 FT-IR spectrometer. A liquid nitrogen-cooled MCT detector was used in all experiments. PMIRRAS offers a number of advantages over other IR techniques, including significantly reduced measurements times, elimination of a background reference scan, virtual elimination of atmospheric water vapor and carbon dioxide interferences and high signal to noise ratio. These advantages allow for characterization of organic layers adsorbed on metal surfaces at low surface concentrations.The freshly prepared samples of BSA and doped –BSA monolayers were mounted in the PMA50 sample holder. The incident beam angle used in all experiments was 85^0. The wavelength setting on a Hinds PEM90 was fixed at 1600cm^{-1} with a half-wave retardation of 0.5. Lock In Amplifier (LIA) SR830 settings, were set according to the PMA50 manual, except for the sensitivity which was set to 5mV or 10mV. The samples were scanned for 10-20 min with 4 cm^{-1} resolution and an aperture setting of 1-1.5mm depending on the signal amplitude. The resulting absorption spectra were recorded between 800 and 4000 cm^{-1}. Conversion of the resulting interferograms to raw PMIRRAS spectra was performed using VisualBasic Script included in Bruker OPUS® Spectroscopy V.5.5 software. Analysis of the raw PMIRRAS spectra, including removal of background, y-scale normalization (using gold substrate spectra) and removal of the LIA gain factor was based on section V.4.E of the PMA50 manual.

7.1 Amide I analysis (de convoultion procedure)

Analysis of protein's secondary structure is based on the assumption that the protein composition can be considered as a linear sum of a few fundamental secondary structures. The analysis of the Amide I band was performed using the curve fitting function of the OPUS® software followed by the interactive least-squares Levenberg Marquardt algorithm. For the initial analysis (un-doped BSA sample), component band's frequency position, width and intensity were all allowed to vary from their initial estimates based on previously reported peak centers[6,7] until the best fit was obtained by the OPUS® software. The resulting frequency position for each peak was then fixed and only the width and intensity were allowed to vary for all subsequent samples of doped BSA. The integrated areas of fitted components, were then normalized to the total Amide-I area, and assumed to be directly proportional to the relative amount of the corresponding secondary structures[6]. Figure S5 shows reprasentative spectra of amide I de-convolution procedure.

7.2 Summary of Amide I and II bands maxima positions

Table S6: Infrared data obtained for self-assembled monolayers of un-doped and doped BSA SAMs

Samples	Amide I maxima cm^{-1}	Amide II maxima cm^{-1}
Un doped BSA	1672 ± 2	1542 ± 1
TPPFeCl doped BSA	1666 ± 7	1539 ± 2
TPPCu doped BSA	1663 ± 8	1536 ± 3

7.3 Representative of Amide I deconvolution procedure (analzyed from PM-IRRAS measurments)

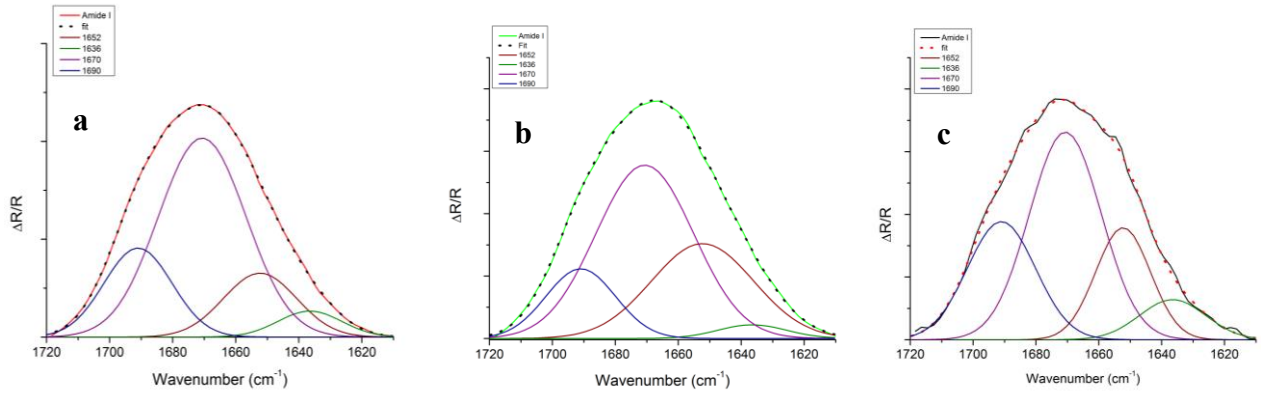

Figure S5 Representative Amide I deconvolution based on a procedure suggested by Desroches et al[6] for (a) undoped BSA (red) (b) TPPCu doped BSA (green) (c) TPPFeCl doped BSA (black) SAMs on gold. Peaks centeres assignemnt [6,7] at 1636cm^{-1} (β– sheet/ extended chains- dark green), 1652cm^{-1} (α– helices-deep purple), 1670 cm^{-1} and 1690 cm^{-1} (β– sheet or β– turn-light purple and blue **)**.

8. References

(1) Schneidman-Duhovny, D.; Inbar, Y.; Nussinov, R.; Wolfson, H. J. *Nucleic Acids Research* **2005**, *33*, W363.

(2) Horcas, I.; Fernandez, R.; Gomez-Rodriguez, J. M.; Colchero, J.; Gomez-Herrero, J.; Baro, A. M. *Review of Scientific Instruments* **2007**, *78*.

(3) Tencer, M.; Charbonneau, R.; Lahoud, N.; Berini, P. *Applied Surface Science* **2007**, *253*, 9209.

(4) Wen, K.; Maoz, R.; Cohen, H.; Sagiv, J.; Gibaud, A.; Desert, A.; Ocko, B. M. *Acs Nano* **2008**, *2*, 579.

(5) Mentovich, E. D.; Belgorodsky, B.; Kalifa, I.; Cohen, H.; Richter, S. *Nano Letters* **2009**, *9*, 1296.

(6) Desroches, M. J.; Chaudhary, N.; Omanovic, S. *Biomacromolecules* **2007**, *8*, 2836.

(7) Roach, P.; Farrar, D.; Perry, C. C. *Journal of the American Chemical Society* **2005**, *127*, 8168.